Available online at www.sciencedirect.com

ScienceDirect

Ceramics International 40 (2014) 2819–2824

CERAMICS INTERNATIONAL

www.elsevier.com/locate/ceramint

Binder removal via a two-stage debinding process for ceramic injection molding parts

Sarizal Md Ani, Andanastuti Muchtar*, Norhamidi Muhamad, Jaharah A. Ghani

Department of Mechanical and Materials Engineering, Faculty of Engineering and Built Environment, Universiti Kebangsaan Malaysia, 43600 UKM Bangi, Selangor, Malaysia

Received 24 July 2013; received in revised form 10 October 2013; accepted 10 October 2013
Available online 21 October 2013

Abstract

Debinding binders in two stages is critical to maintaining the shape of injected parts; the resulting decomposition affects the strength and rigidity of a structure. This study determines the optimal debinding process on the basis of a higher binder removal rate and the production of defect-free parts. The feedstock used was a combination of alumina–zirconia powder with a binder that consists of high-density polyethylene (HDPE), paraffin wax (PW), and stearic acid (SA). During the first stage, the injected parts were immersed in an *n*-heptane solution at 50 °C, 60 °C, 65 °C, and 70 °C to remove PW and SA. Binder weight loss was evaluated as a function of time. In the second stage, HDPE was removed by using thermal debinding. The results show that the optimum solvent debinding process runs for 16 h at 60 °C. The weight loss of the binder reaches 41.1% and results in the formation of defect-free parts. The binders are degraded at approximately 550 °C during thermal debinding. This degradation resulted in decomposition of nearly 96.9% of the binders. Low heating rates (1 °C/min to 2 °C/min) prevent defects from forming in the injected parts.

Keywords: A. Injection molding; C. Diffusion; Debinding; Alumina–zirconia

1. Introduction

Ceramic injection molding (CIM) is a combination of powder technology and injection molding. The CIM process is a near-net shape processing technique that facilitates the low-cost manufacture of ceramic components with complex shapes [1–3]. The CIM process involves several stages, namely, mixing, injection molding, debinding, and sintering. German and Bose [4] described debinding as a process in which a binder is removed from injected parts, thereby producing commonly designated brown parts. The process must be carefully performed to avoid problems that affect quality, such as component distortion, cracking, blistering, and contamination of parts. Debinding involves a long processing period, thereby prompting the development of different debinding techniques, including solvent, thermal, wicking, evaporation and catalytic debinding, as well as the combination of these approaches [5,6].

The use of a multi-component binder system enables two-stage binder removal. German [7] and Liu et al. [8] stated that binder removal in two stages is important in avoiding defects in the shape of parts and in reducing total debinding time. The main binder (backbone component) is usually a thermoplastic that maintains the shape of the injected parts by confining ceramic powder particles, which are then thermally removed during the second debinding stage. Moreover, the support binder (commonly a wax), which functions as a filler phase, is eliminated during the first debinding stage by immersing the injected part in a solvent, such as heptane, hexane, and kerosene. The low decomposition temperature and molecular weight of the support binder facilitate debinding at the first stage, as reported by Iriany [9] and Krauss et al. [10]. Furthermore, pore channels that are formed as a result of filler removal enable the main binder to seep out of the body structure [11,12].

Cheng et al. [13] and Thomas-Vielma et al. [14] showed that combining solvent and thermal debinding techniques successfully

*Corresponding author. Tel.: +60389118379; fax: +60389118314.
E-mail addresses: sarizal@eng.ukm.my (S. Md Ani), muchtar@eng.ukm.my, tutimuchtar@gmail.com (A. Muchtar), hamidi@eng.ukm.my (N. Muhamad), jaharah@eng.ukm.my (J.A. Ghani).

0272-8842/$ - see front matter © 2013 Elsevier Ltd and Techna Group S.r.l. All rights reserved.
http://dx.doi.org/10.1016/j.ceramint.2013.10.032

reduces binder decomposition time and prevents defects from forming in injected parts. However, few researchers have discussed a debinding process that involves the combination of alumina and zirconia ceramic powder with a binder that consists of high-density polyethylene (HDPE), paraffin wax (PW), and stearic acid (SA). In the current study, an *n*-heptane solution was used to dissolve PW and SA during the first debinding stage, and HDPE was removed by thermal debinding during the second stage. The debinding profile for thermal elimination was optimized through thermogravimetric analysis (TGA) of the binder. This study attempted to determine the optimal debinding process based on higher binder removal rate and production of defect-free parts in a multi-component binder system.

2. Materials and methods

2.1. Materials

The feedstock used in this study was a mixture of alumina and zirconia (3 mol% yttria) powders combined with a multi-component binder system composed of HDPE, PW, and SA. The mixture was 80 wt% alumina powder and 20 wt% zirconia powder. The alumina powder (AL-160SG-1), which has an average particle size of 0.40 μm and a specific surface area of 7.0 m^2/g, was supplied by Showa Denko. The zirconia powder (KZ-3YF), which has an average particle size of 0.35 μm and a specific surface area of 9.0 m^2/g, was supplied by KCM Corporation. Before mixing, the ceramic powder was dried for 1 h in an electric furnace at 110 °C. The alumina and zirconia powders were then mixed by using dry mixing, which was performed at 100 rpm for 8 h by using a ball mill. The ball-to-powder ratio was 5:1. The average size and density of the alumina–zirconia powder after dry mixing were 0.31 μm and 4.46 g/cm^3, respectively. The morphology of the alumina–zirconia powder is shown in Fig. 1. Table 1 shows the characterization results for the binders. Differential scanning calorimetry (DSC) analysis and TGA were conducted to determine the melting and decomposition temperatures of the binders. DSC and TGA were performed on a Mettler Toledo DSC 1 STAR^e System and Netzsch STA 449 F3 Jupiter at a heating rate of 10 °C/min.

2.2. Feedstock preparation and injection molding

The alumina–zirconia powder was mixed with the binders by using an internal mixer machine (Brabender W 50 EHT) to produce the feedstock. Mixing was conducted at 140 °C with 20 rpm velocity for 30 min. The alumina–zirconia powder loading was 57 vol% (86.5 wt%), and the binder composition was 50 wt% HDPE, 46 wt% PW, and 4 wt% SA. The composition and combination of the binders were based on the method proposed by Thomas-Vielma et al. [14]. The feedstock, which was appropriately granulated after mixing (Strong Crusher TSC-5JP), consisted of 18.09 wt% carbon, 30.63 wt% oxygen, 36.74 wt% alumina, and 14.54 wt% zirconia. The elemental content, which refers to the average percent of elements with different batches of mixing, was determined by using energy dispersive X-ray spectroscopy (EDX) associated with field emission scanning electron microscopy (SEM) (Hitachi SU8020 FESEM). An SEM image of the feedstock is shown in Fig. 2. A standard screw-type injection molding machine (Battenfeld BA 250 CDC) was used to produce the injected parts. The mold cavity was characterized by a round bar (∅15 × 21 mm^2). The injection temperature and pressure were 160 °C and 110 MPa, respectively. The injection and holding times were 5 s and 10 s, respectively, and the molding temperature was 50 °C. The injection molding conditions were optimized according to previous research [15].

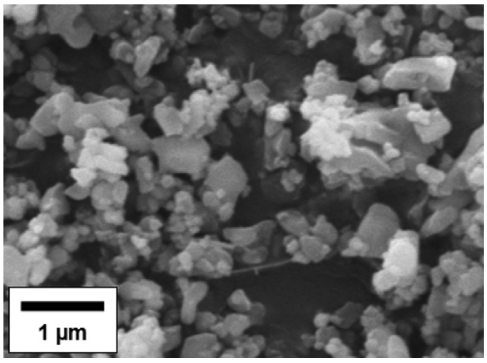

Fig. 1. Morphology of the alumina–zirconia powder.

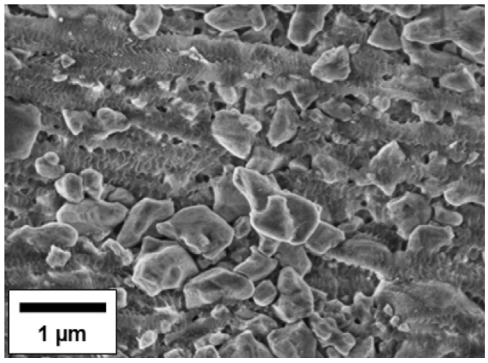

Fig. 2. SEM image of the feedstock.

Table 1
Characterization of the binders.

Binder	Supplier	Chemical structure	Density (g/cm^3)	Melting temperature (°C)	Decomposition temperature (°C)
HDPE	Titan petchem	$(–CH_2–CH_2–)_n$	0.96	131.8	420–550
PW	Emercy oleochemicals	$C_{31}H_{64}$	0.89	59.5	200–400
SA	Emercy oleochemicals	$C_{18}H_{36}O_2$	0.88	69.8	180–380

2.3. Debinding process

A two-stage debinding process, which is a combination of solvent and thermal debinding, was adopted to remove the multi-component binder system in the injected parts. Solvent debinding was performed by immersing the injected parts in an *n*-heptane (Merck 104379) solution at different temperatures for specific periods. The temperature ranged from 50 °C to 70 °C (Medcenter Venticell III), and the injected parts were immersed in the solution every 2 h. The sample was subsequently dried before weighing to obtain the percentage weight loss of the binder. Thermal debinding was then performed by heating the injected parts in a purified argon atmosphere. The gas pressure in the furnace (Maju Saintifik RS800/200/200) was fixed at 1 kg/cm^2. The thermal debinding profile was designed in accordance with the TGA of the binders. The sample was re-weighed to determine the percentage weight loss of all the binders after thermal elimination. The defects of the debound parts were observed by using an Olympus Stereomicroscope SZ6. The microstructure and elemental content were examined by using SEM and EDX (Zeiss Evo MA10 VPSEM and Hitachi SU8020 FESEM).

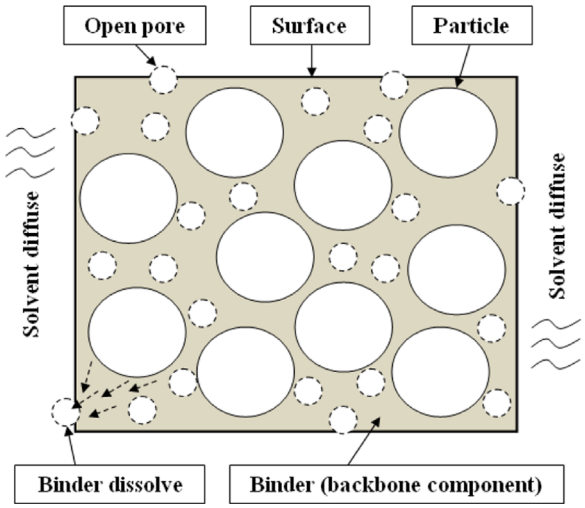

Fig. 3. Schematic of the solvent debinding process.

3. Results and discussion

3.1. Solvent debinding

The debinding of the injected parts was implemented in two stages: solvent and thermal debinding. During the first stage, solvent debinding was performed by immersing the injected parts in an *n*-heptane solution at different temperatures and immersion periods. This method was selected because PW and SA can be dissolved through immersion in *n*-heptane, thereby allowing the solubility of *n*-heptane to approach that of the binder component [9]. This process produced a porous injection part, which facilitated HDPE diffusion into the second debinding stage. Fig. 3 shows a schematic view of the solvent debinding process, as well as the condition of the support binder, which was removed from the injected part because of capillary forces that occurred when these parts began to dissolve in the *n*-heptane solution; this process was discussed by German [16]. The melting point of the binders, which is the indicator for the selection of solvent temperature during debinding, was tested by using DSC analysis (Fig. 4). During heating, the peak melting temperatures of the multi-component binder system were 60.2 °C and 127.6 °C. Low melting temperatures were applied to the PW and SA binder components, whereas a high melting temperature was applied to HDPE. The solubility and diffusivity of the binders in the solvent (*n*-heptane) were directly affected by temperature. Therefore, the temperature for solvent debinding was determined on the basis of the melting temperatures of the binders. During the first debinding stage, the melting temperatures of PW and SA were used as reference. The combination of PW and SA represented half of the binder content. Based on such composition, the weight loss of the binder during the first stage reached up to 50 wt%.

Fig. 5 shows the effect of immersion time and solvent temperature on the weight loss percentage of the binder. The changes in these parameters considerably affected the percentage of the binders that diffused from the injected parts. When an injected part was soaked in the solvent at a prolonged period, more binders were removed. The debinding rate was significantly faster in the early stages because the binder was in

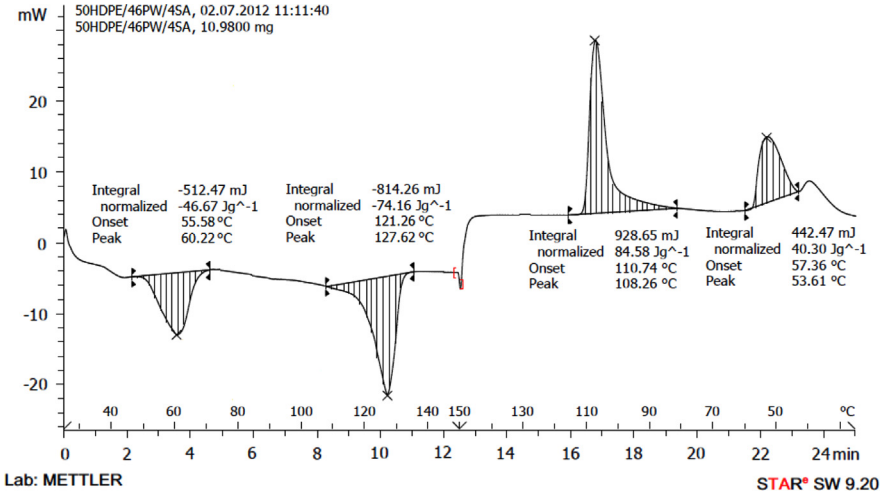

Fig. 4. Differential scanning calorimetry curve of the multi-component binder system.

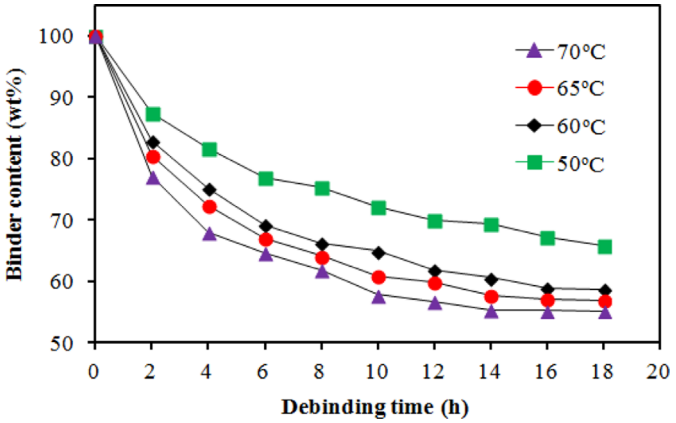

Fig. 5. Effect of solvent temperature on the weight loss of binders at various immersion times.

direct contact with the solvent. Subsequently, the solvent diffused deeply into the injected part before it dissolved the binder. Therefore, the debinding rate substantially slowed until it reached a plateau after 16 h. The weight loss of the binders remained nearly unchanged because a dynamic equilibrium between the binders and solvent was reached; this phenomenon was described by Cheng et al. [13]. In addition, Iriany [9] reported that the diffusion process is affected by the microstructure layout of injected parts. Binders cannot be completely eliminated in case of dead ends because the porous channel in microstructures does not interconnect with others. Fig. 6 shows the SEM microstructure of the injected parts after being immersed in the *n*-heptane solution at 60 °C at different immersion times. At this temperature, the injected parts were free from defects. The increase in immersion time eliminated substantial amounts of PW and SA, thereby forming a more porous structure (as shown in Fig. 6c). Therefore, empty spaces existed between the ceramic powder and HDPE.

Increase in solvent temperature accelerates debinding. At a high temperature, the binders rapidly melt, and the rate of solvent diffusion increases. Experimental results show that at an immersion time of 2 h, nearly 12.6 wt% and 17.2 wt% of the binder (PW and SA) were eliminated at 50 °C and 60 °C, respectively. Up to 19.6 wt% and 22.9 wt% of the binders were successfully removed at immersion temperatures of 65 °C and 70 °C, respectively. However, a very high immersion temperature was less suitable for solvent debinding because it caused defects in the injected parts. According to Murtadhahadi [17] and Tsai and Chen [18], at a high temperature (exceeding the melting point of a binder), more binders are melted and diffused rapidly out of the body structure. This situation causes defects in the injected parts. However, German and Bose [4] associated cracking to the swelling of the injected part, which was due to thermal expansion of the binders as a result of the reaction between the solvent and the binders at a higher temperature. In the present study, cracking occurred after immersion at 65 °C and 70 °C. Cracks initially formed after 2 h of immersion at a higher temperature. Fig. 7 shows the cracking of the sample after immersion at 65 °C. Thus, the optimal solvent debinding process occurred at 60 °C given the high weight loss of the binder. After

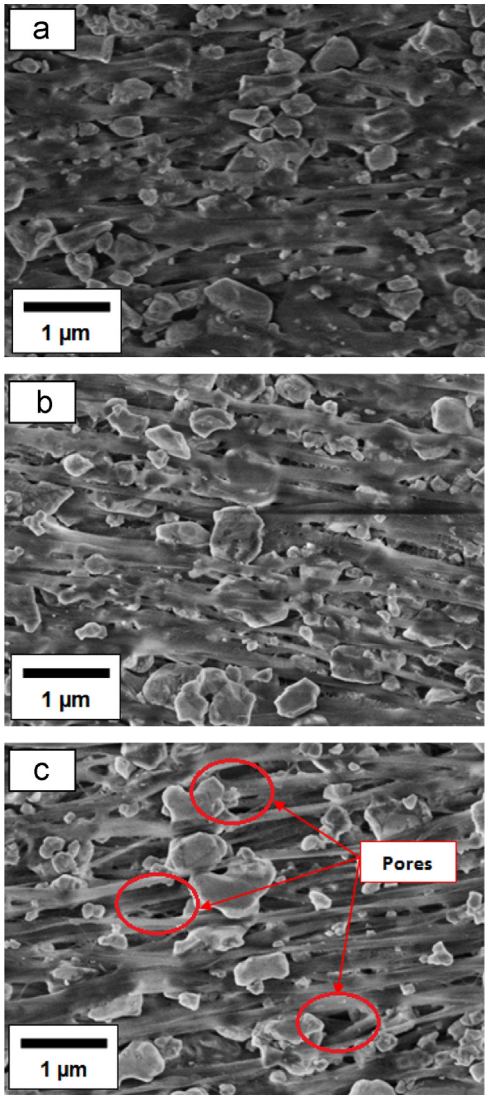

Fig. 6. SEM images of the injected parts after solvent debindingat 60 °C for (a) 0 h, (b) 4 h, and (c) 16 h.

16 h of immersion, the weight loss of the binder reached 41.5%, which resulted in the formation of defect-free parts.

3.2. Thermal debinding

Solvent debinding was followed by thermal debinding. The debinding profile for thermal elimination was optimized on the basis of the TGA of the binders. Fig. 8 shows the TGA results for the feedstock and pure binders at a heating rate of 10 °C/min in purified argon at a temperature range of 30 °C–600 °C. The pure binders decomposed in one step; however, the multi-component binder system in the feedstock required an additional step in the process. The PW and SA decomposed at approximately 180 °C–200 °C and were completely eliminated at approximately 380 °C–400 °C. The main binder, HDPE, decomposed once the temperature exceeded 420 °C and was completely decomposed at approximately 550 °C. The multi-component binder system gradually decomposed at a wide temperature range, beginning at 180°C and completely

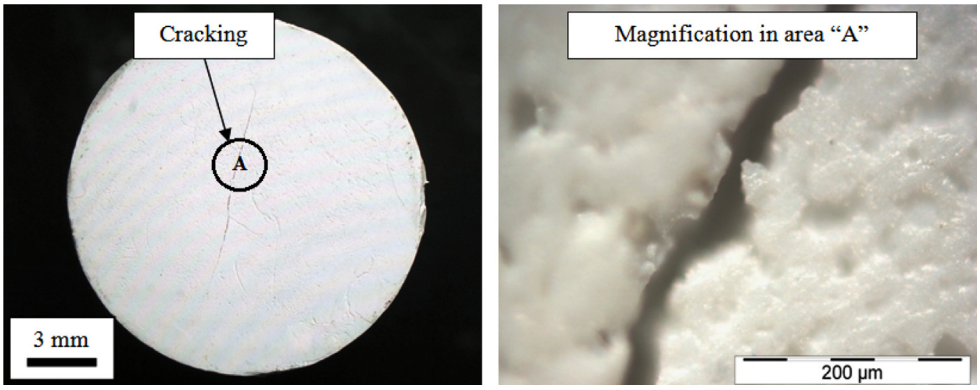

Fig. 7. Images of cracks after solvent debinding at 65 °C

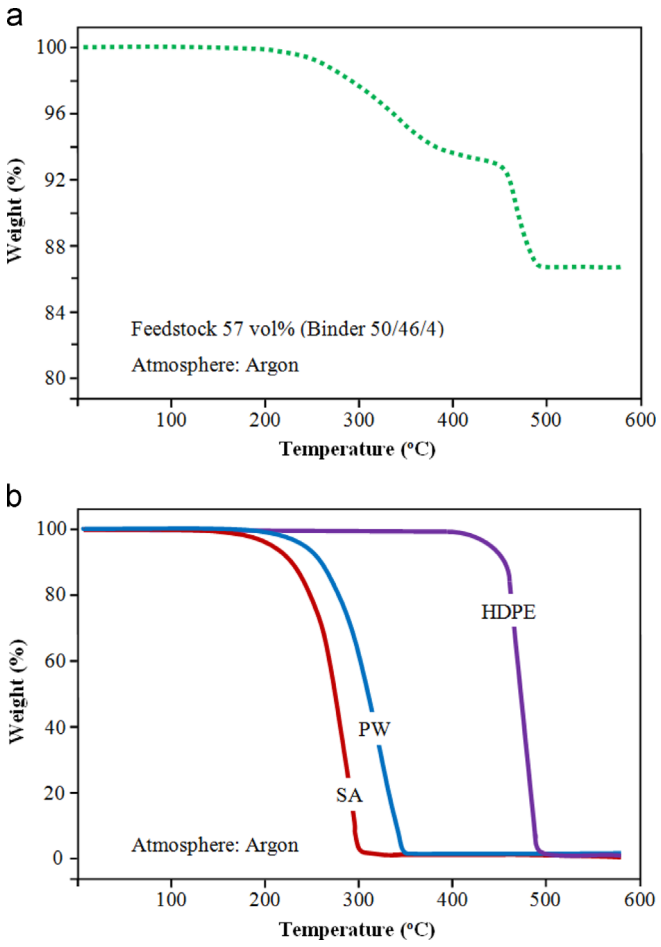

Fig. 8. Thermogravimetric analysis of the (a) feedstock and (b) pure binders.

decomposing at approximately 550 °C. This wide temperature range during thermal debinding helps to prevent defect formation and leaves behind a porous channel to allow the outflow of gaseous matter [13].

Fig. 9 shows the optimized thermal debinding profile. At the first stage, a heating rate of 2 °C/min was used from room temperature and increased to 420 °C. At this point, the PW and SA residuals were completely eliminated, thereby forming a porous structure. At a temperature range of 420 °C–550 °C, a slower heating rate was employed, which triggered the decomposition of

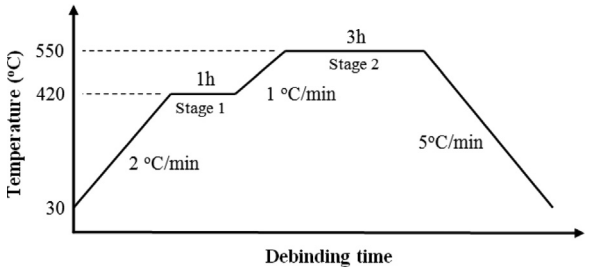

Fig. 9. Optimized thermal debinding profile.

the HDPE binder. Decomposition gases were released through the porous body structure. Thomas-Vielma et al. [14] revealed that a high heating rate can cause pressure build-up and temperature gradients inside the injected parts. This situation can form defects, such as cracking and blistering, in the injected parts. Fig. 10a shows the SEM image of the injected parts at the second debinding stage with a 1 h holding time. Experimental results show that nearly 90.5 wt% of the binder was decomposed. The relatively large sizes of the injected parts resulted in HDPE residues, which can be observed at the center of the injected parts, as shown in Fig. 10b. After the holding time was extended to 3 h, nearly 96.9 wt% of the binder was successfully removed (Fig. 11). According to Mohd Foudzi et al. [3], the remaining binder of 2 wt%–6 wt% was used to sustain the shape prior to sintering. The sizes of the injected parts did not change significantly after solvent debinding due to the higher of powder loading. After debinding, the elemental content of the injected parts included 2.77 wt% carbon, 40.29 wt% oxygen, 41.24 wt% alumina, and 15.70 wt% zirconia. The results show that the available carbon content decreases; since the majority of the binders originally consisted of the carbon element. The remaining binder was completely removed after sintering.

4. Conclusions

Two-stage debinding was performed to determine the optimal debinding process for injected parts. Temperature and immersion time significantly affect binder weight loss during solvent debinding. Immersion at 60 °C for 16 h is considered the optimum condition for solvent debinding

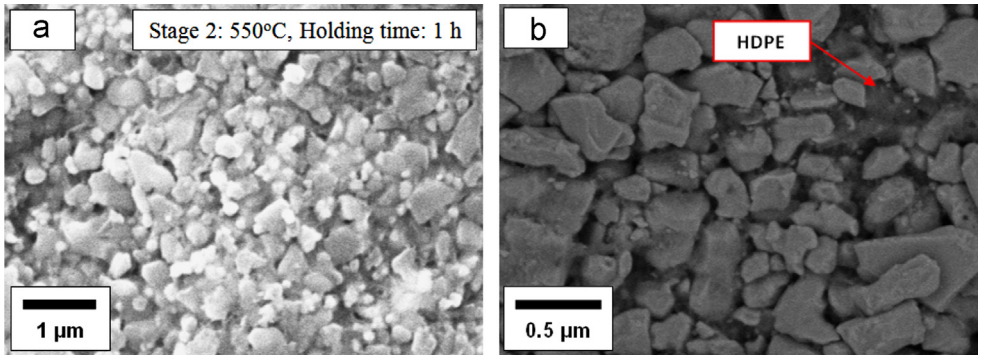

Fig. 10. SEM images of (a) the injected part after thermal debinding at 1 h holding time and (b) the residue of HDPE.

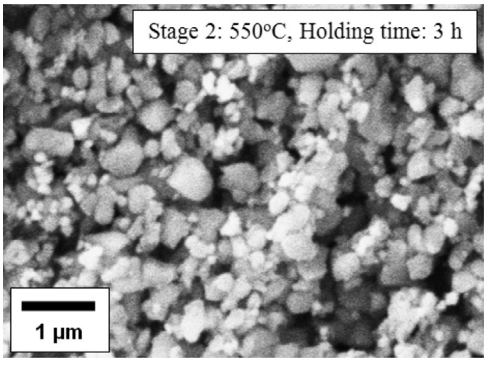

Fig. 11. SEM image of the injected part after thermal debinding at 3 h holding time.

because of the increased rate of binder weight loss and the resulting defect-free parts. Moreover, TGA of the data facilitates acquisition of the optimal thermal debinding profile. During thermal debinding, nearly 96.9% of the binder is removed. Low heating rate and a long holding time allow complete diffusion of the binders. All the binders in the injected parts are successfully eliminated by the combination of solvent and thermal debinding techniques, thereby preventing the formation of defects in the injected parts.

Acknowledgments

The authors acknowledge the Universiti Kebangsaan Malaysia (UKM) and the Malaysian Government for their sponsorship under (Grants nos. UKM-AP-NBT-14–2010 and GUP-2012-060). The first author also acknowledges Japan–Malaysia Technical Institute and the Public Service Department of Malaysia for their support on the author's graduate studies.

References

[1] F.A. Cetinel, W. Bauer, M. Muller, R. Knitter, J. Haubelt, Influence of dispersant, storage time and temperature on the rheological properties of zirconia–paraffin feedstocks for LPIM, J. Eur. Ceram. Soc. 30 (2010) 1391–1400.

[2] B. Loebbecke, R. Knitter, J. Haubelt, Rheological properties of alumina feedstocks for the low pressure injection moulding process, J. Eur. Ceram. Soc. 29 (2009) 1595–1602.

[3] F. Mohd Foudzi, N. Muhamad, A.B. Sulong, H. Zakaria, Yttria stabilized zirconia formed by micro ceramic injection molding: rheological properties and debinding effects on the sintered part, Ceram. Int. 39 (2013) 2665–2674.

[4] R.M. German, A. Bose, Injection Molding of Metals and Ceramics, Princeton, New Jersey, Metal Powder Industries Federation, 1997.

[5] H.R.C. Silva Jorge, Compounding and processing of a water soluble binder for powder injection moulding (Ph.D. thesis), Universidade do Minho, 2008.

[6] M. Trunec, J. Cihlar, Thermal removal of multicomponent binder from ceramic injection mouldings, J. Eur. Ceram. Soc. 22 (2002) 2231–2241.

[7] R.M. German, Powder Injection Molding, Princeton, New Jersey, Metal Powder Industries Federation, 1990.

[8] Z.Y. Liu, N.H. Loh, S.B. Tor, K.A. Khor, Y. Murakoshi, R. Maeda, Binder system for micropowder injection molding, Mater. Lett. 48 (2001) 31–38.

[9] Iriany, Rheological study of metal injection molding feedstock containing palm stearine (Ph.D. thesis), Universiti Kebangsaan Malaysia, 2002.

[10] V.A. Krauss, A.A.M. Oliveira, A.N. Klein, H.A. Al-Qureshi, M. C. Fredel, A model for PEG removal from alumina injection moulded parts by solvent debinding, J. Mater. Process. Technol. 182 (2007) 268–273.

[11] N.H. Loh, S.B. Tor, K.A. Khor, Production of metal matrix composite part by powder injection molding, J. Mater. Process. Technol. 108 (2001) 398–407.

[12] T. Moritz, R. Lenk, Ceramic injection moulding: a review of developments in production technology, materials and applications, Powder Inject. Mould. Int. 3 (2009) 23–34.

[13] J. Cheng, W. Lei, C. Yanbo, Z. Jinchuan, S. Peng, D. Jie, Fabrication of w–20wt.%cu alloys by powder injection molding, J. Mater. Process. Technol. 210 (2010) 137–142.

[14] P. Thomas-Vielma, A. Cervera, B. Levenfeld, A. Varez, Production of alumina parts by powder injection molding with a binder system based on high density polyethylene, J. Eur. Ceram. Soc. 28 (2008) 763–771.

[15] S.M. Ani, A. Muchtar, N. Muhamad, J.A. Ghani, Effects of injection temperature and pressure on green part density for ceramic injection molding, Adv. Mater. Res. 622–623 (2013) 429–432.

[16] R.M. German, Theory of thermal debinding, Int. J. Powder Metall. 23 (1987) 237–245.

[17] Murtadhahadi, Injection parameter for metal injection molding (MIM) process to make use of feedstock of SS 316 L, PEG, PMMA and stearic acid (M.Sc. thesis), Universiti Kebangsaan Malaysia, 2007.

[18] D.S. Tsai, W.W. Chen, Solvents debinding kinetics of alumina green bodies by powder injection molding, Ceram. Int. 21 (1995) 257–264.